Jpn. J. Appl. Phys. Vol. 39 (2000) pp. L 503–L 505
Part 2, No. 6A, 1 June 2000

First Fabrication of GaInAs/InP Buried Metal Heterojunction Bipolar Transistor and Reduction of Base-Collector Capacitance

Toshiki ARAI, Yoshimichi HARADA, Shigeharu YAMAGAMI, Yasuyuki MIYAMOTO* and Kazuhito FURUYA
Department of Electrical and Electronic Engineering, Tokyo Institute of Technology, 2-12-1 O-okayama, Meguro-ku, Tokyo 152-8552, Japan

(Received April 3, 2000; accepted for publication April 19, 2000)

We report a novel approach for improving the performance of InP-based heterojunction bipolar transistors (HBTs). A buried-metal heterojunction bipolar transistor (BM-HBT), in which tungsten stripes of the same area as the emitter metal were buried in an i-InP collector layer, was fabricated for the first time. The aim in fabricating this structure is to realize a reduction in the total base-collector capacitance (C_{BCT}). In the measurement of microwave S-parameters, C_{BCT} of 10.3 fF was evaluated. The effective base-collector junction area of the BM-HBT was estimated to be 22% that of conventional-HBT considering the difference in collector thickness.

KEYWORDS: InP, GaInAs, tungsten, HBT, BM-HBT, C_{BC}, OMVPE

1. Introduction

In heterojunction bipolar transistors (HBTs), reduction of the total base-collector capacitance (C_{BCT}) is very important for high-speed operation, because it increases the current gain cutoff frequency (f_T) and enhances maximum stable/available gain (MSG/MAG) at frequencies below the maximum oscillation frequency (f_{max}).[1] C_{BCT} comprises the internal base-collector capacitance (C_{BCin}) and external base-collector capacitance (C_{BCex}). C_{BCex} is defined by the area of the extrinsic base region. In the conventional HBT, C_{BCin} decreases in proportion to decreasing emitter size, but C_{BCex} does not decrease. Therefore, the improvement of RF characteristics reaches a ceiling even if the emitter width is further reduced. To reduce C_{BCT} of HBTs, implanted base extrinsic regions,[2] undercutting collector and subcollector layers,[3] a buried subcollector using selective growth[4] and a transferred-substrate process[5] have been previously demonstrated. In addition, we proposed the buried metal heterojunction bipolar transistor (BM-HBT).[6] We selected an InP-based system for fabricating BM-HBT since the electric properties of GaInAs that is lattice-matched to InP are superior to those of GaAs.

In this paper, we report the first-time fabrication of GaInAs/InP BM-HBT. In the observation of the cross section, the absence of void formation around the buried tungsten and the exact alignment of the emitter mesa with the buried collector electrode were confirmed. C_{BCT} was calculated from the measurement of S-parameters. An effective reduction of C_{BCT} was confirmed by comparison with conventional HBT.

2. Experiments

Figure 1 shows the schematic view of BM-HBT. Active layers of BM-HBT consist of a double hetero-structure. Metal wires with an area equal to that of the emitter mesa are formed on the semi-insulating InP substrate. These are buried by an i-InP layer upon the growth of the HBT layers. The buried metal wires are in contact with the i-InP collector layer and operate as a Schottky collector electrode. There is no conductive layer under the extrinsic base region. Therefore, the reduction of C_{BCT} is achieved.

The embedded metal should not form an alloy with the compound semiconductor at the growth temperature of organometallic vapor phase epitaxy (OMVPE). It was confirmed that tungsten fulfilled this requirement.[7,8] Thus, we selected tungsten for the buried metal. When a metal embedded in semiconductor is used for the electron devices, no void formation around the buried metal and a flat top surface are required. Buried growth by an InP layer over tungsten stripes using OMVPE has been previously reported.[9] As a result, we obtained the growth conditions for satisfying these requirements and the stripes of 1 μm width and 2 μm period were buried by a 1-μm-thick InP layer. In the calculation of the RF characteristics of BM-HBT, the estimated collector thickness for the highest f_{max} is about 300 nm.[6] Thus the width of the buried wires must be less than 300 nm. In the case of fabrication using a 2-μm-wide emitter applying a conventional process, many tungsten wires of fine width must be buried under the emitter.

We fabricated the devices with emitter widths of 2 μm and 3 μm. We initiated the fabrication process by forming tungsten stripes on the semi-insulating InP substrate. The tungsten stripes were formed by the metal-stencil liftoff process using electron beam lithography.[9] The total widths of the stripes were 2 μm and 3 μm. The width, thickness and length of the wires were 100 nm, 40 nm and 16 μm, respectively. The wires were set with a period of 200 nm. The stripes were oriented at an angle of 45° from $\langle 01\bar{1} \rangle$. At the same time, a tungsten mark for alignment of the emitter with the buried tungsten stripes was formed. Next, the crystal layers were grown on the sample by OMVPE where the subcollector was removed from

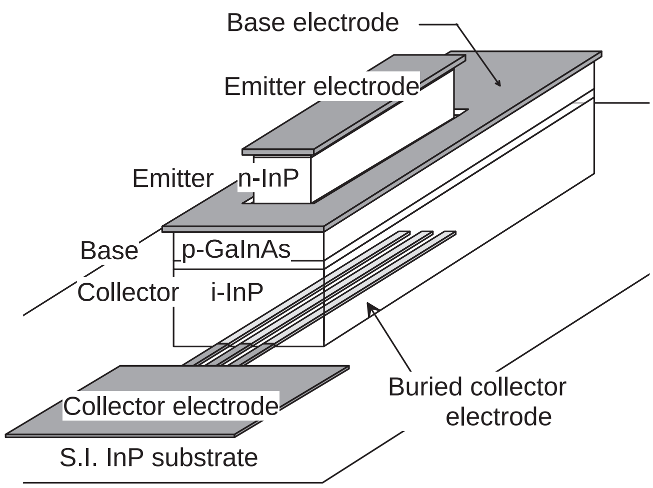

Fig. 1. Schematic view of the fabricated BM-HBT.

*E-mail address: miya@pe.titech.ac.jp

Table I. Layer structure parameters of the BM-HBT.

Layer	Material	Doping [cm^{-3}]	Thickness [nm]
Contact	n-GaInAs	2×10^{19}	20
Emitter	n-InP	2×10^{19}	70
	n-InP	5×10^{17}	100
Base	p-GaInAs	2×10^{19}	50
Collector	i-GaInAs	—	40
	i-GaInAsP	—	20
	n-InP	5×10^{17}	5
	i-InP	—	230

typical DHBTs. The layer structures are shown in Table I. Trimethylindium and triethylgallium as group III materials, and phosphine and arsine as group V materials were used. The growth temperatures were 600°C, 500°C and 565°C for the collector layers, base layer and emitter layer, respectively. The growth conditions optimized for the buried growth of the InP collector layer were a growth temperature of 600°C, V/III ratio of 460 and growth rate of 28 nm/min.[9] Next, the mesa structure was formed by wet chemical etching and patterned by photolithography. The InP layers were etched by a HCl:H_3PO_4=1 : 1 solution, while the GaInAs layers and the GaInAsP layer were etched by a citric acid:H_2O_2=5 : 1 solution. An emitter electrode was formed in alignment with the buried tungsten stripes. A base electrode was formed by a self-alignment technique. The areas of the emitter and base electrode were $2 \times 10\,\mu m^2$ and $6 \times 16\,\mu m^2$, respectively. The emitter and base metals were Ti/Pt/Au. The device was isolated by the formation of a base mesa. At the same time, a part of the buried tungsten stripes was exposed for connection. A collector electrode was formed on the stripes. The device was embedded by polyimide for planarization and passivation. After opening of the contact windows using reactive ion etching, Cr and Au were evaporated for the interconnection.

3. Results and Discussions

Figure 2 shows the common-emitter collector *I–V* characteristics of a device with a 2-μm-wide emitter. The current gain was about 70 at the collector voltage (V_C) of 4 V. Microwave *S*-parameters were measured from 50 MHz to 30 GHz using an HP8722 network analyzer. Extrapolations of f_T and f_{max} were carried out from the −20 dB/decade regions of current gain ($|h_{21}|^2$) and Mason's unilateral gain (U), respectively. In the measurement of the dependence of f_T and f_{max} on collector current (I_C), the values of f_T and f_{max} reached peak points ($f_T = 33.5$ GHz, $f_{max} = 47.3$ GHz) at $I_C = 4$ mA and $V_C = 6$ V.

The C_{BCT} of 10.3 fF was calculated from the imaginary part of Y_{12} parameters in a low-frequency region. We also fabricated a conventional HBT with almost the same planar dimensions as a reference. The measured C_{BCT} was 53 fF when the collector thickness was 260 nm. C_{BCT} values of BM-HBT and conventional HBT could not be compared with each other directly, because C_{BCT} depends on collector layer thickness. To measure the collector layer thickness of fabricated devices, BM-HBT was cut by a focused ion beam. A cross-sectional SEM view of the fabricated device with emitter width of 3 μm is shown in Fig. 3. It was confirmed that the emitter mesa was aligned with the buried tungsten stripes and no void was formed around the buried tungsten. The measured collector thickness was 290 nm. The effective base-collector junction area (S_{BCJ}) was calculated from C_{BCT} considering the difference in the collector layer thickness. A two parallel plate model was used. We assumed that the intrinsic layer of the collector was completely depleted. S_{BCJ} values of BM-HBT and conventional-HBT were 26 μm^2 and 119 μm^2, respectively. Thus, we achieved a BM-HBT in which the effective base-collector junction area was 22% that of conventional HBT.

The emitter resistance (R_{EE}) of 15 Ω was measured using the open collector method. However, the collector resistance (R_{CC}) could not be measured using the open emitter method, because the interface between the collector layer and the collector metal formed a Schottky junction and the base-collector junction did not operate as a p-n diode. The value of

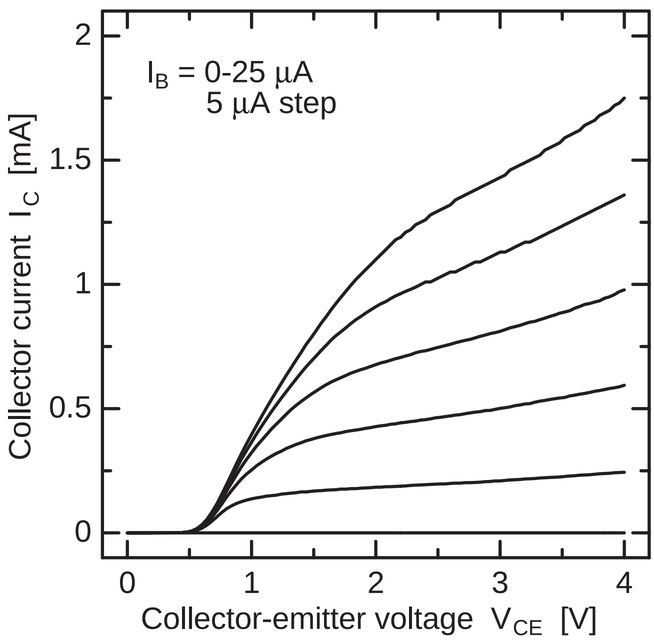

Fig. 2. Common-emitter collector *I–V* characteristics of BM-HBT with an emitter area of $2 \times 10\,\mu m^2$.

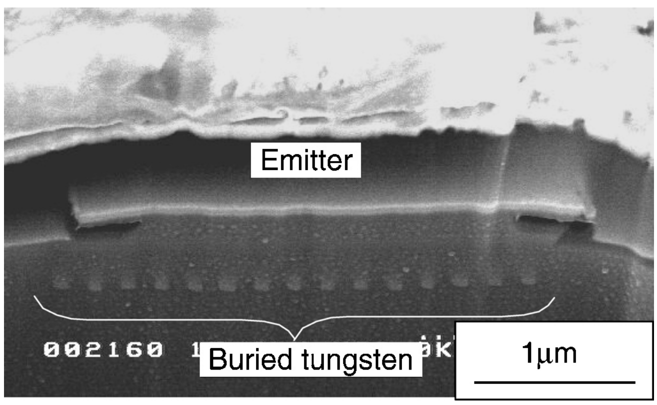

Fig. 3. A SEM view of a cross section cut by a focused ion beam. Measured collector thickness was 290 nm.

$R_{EE} + R_{CC}$ estimated from the linear region of the common-emitter collector I–V characteristics was about 400 Ω. Thus, R_{CC} was estimated to have a high value.

Because the collector junction of BM-HBT was biased as a forward Schottky junction, the contact resistance between the collector layer and collector metal must be sufficiently small. Thus, we assumed that the high R_{CC} was due to the high resistivity of tungsten. To measure the resistivity, other samples were fabricated. The fabrication process was similar to that used for forming the buried tungsten stripes and interconnection in BM-HBT. As a result, the estimated resistivity was 160 $\mu\Omega$ cm. The value of R_{CC} calculated using this resistivity was 360 Ω and the reason for the high resistance was explained. The resistivity of tungsten was strongly dependent on the sample temperature at evaporation[10] and a value less than 10 $\mu\Omega$ cm was reported when the temperature was about 200°C.[11] In the fabrication process of BM-HBT, the sample holder was cooled to 0°C to prevent deformation of the resist pattern. Thus, optimization of the fabrication process will overcome the high resistivity of tungsten, resulting in high-speed operation of BM-HBT.

4. Conclusion

GaInAs/InP-based BM-HBT with an emitter area of $2\times10\,\mu m^2$ was successfully fabricated for the first time. S-parameters were measured to indicate f_T of 33.5 GHz and f_{max} of 47.3 GHz at I_C of 4 mA. S_{BCJ} of BM-HBT was 22% that of conventional HBT and C_{BCT} was effectively reduced in BM-HBT. This result showed the possibility of high performance of BM-HBT.

Acknowledgements

The authors would like to thank Professor S. Arai, Professor M. Asada and Associate Professor M. Watanabe for helpful discussions and encouragement. This work was supported by the Ministry of Education, Science, Sports and Culture through a Scientific Grant-In-Aid, and the Research Center for Ultra-High-Speed Electronics and by the "Research for the Future" Program #JSPS-RFTF96P00101 of the Japan Society for the Promotion of Science (JSPS).

1) K. Kurishima: IEEE Trans. Electron Device **43** (1996) 2074.
2) P. M. Asbeck, D. L. Miller, R. J. Anderson and F. H. Eison: IEEE Electron Device Lett. **EDL-5** (1984) 310.
3) Y. Miyamoto, J. M. M. Rios, A. G. Dentai and S. Chandrasekhar: IEEE Electron Device Lett. **17** (1996) 97.
4) M. R. Frei, J. R. Hayes, J.-I. Song, H. M. Cox and C. Caneau: Appl. Phys. Lett. **61** (1992) 1193.
5) U. Bhattacharya, M. J. Mondry, G. Hurts, I.-H. Tan, R. Pullela, M. Reddy, J. Guthrie, M. J. W. Rodwell and J. E. Bowers: IEEE Electron Device Lett. **16** (1995) 357.
6) T. Arai, H. Tobita, Y. Harada, M. Suhara, Y. Miyamoto and K. Furuya: *Proc. 11th Int. Conf. Indium Phosphide & Related Materials, Davos, Switzerland, 1999* (IEEE, Piscataway, 1999) p. 183.
7) H. Hongo, Y. Miyamoto, J. Suzuki, M, Funayama, T. Morita and K. Furuya: Jpn. J. Appl. Phys. **33** (1994) 925.
8) M. Suhara, L.-E. Wernersson, B. Gustafson, N. Carlsson, W. Seifert, A. Gustafsson, J.-O. Malm, A. Litwin, A. Samuelson and K. Furuya: Jpn. J. Appl. Phys. **38** (1999) 3466.
9) T. Arai, H. Tobita, Y. Harada, M. Suhara, Y. Miyamoto and K. Furuya: to be published in Physica E.
10) K. Y. Ahn: Thin Solid Films **150** (1987) 469.
11) R. L. Krans, A. Berntsen and W. C. Sinke: Mater. Res. Soc. Symp. Proc. **181** (1990) 597.